PHOTONICS Research

Program-controlled single soliton microcomb source

Xinyu Wang,[1,2] Peng Xie,[1,2] Weiqiang Wang,[1,2,4] Yang Wang,[1,2] Zhizhou Lu,[1,2] Leiran Wang,[1,2] Sai T. Chu,[3] Brent E. Little,[1,2] Wei Zhao,[1,2] and Wenfu Zhang[1,2,5]

[1]State Key Laboratory of Transient Optics and Photonics, Xi'an Institute of Optics and Precision Mechanics (XIOPM), Chinese Academy of Sciences (CAS), Xi'an 710119, China
[2]University of Chinese Academy of Sciences, Beijing 100049, China
[3]Department of Physics and Materials Science, City University of Hong Kong, Hong Kong, China
[4]e-mail: wwq@opt.ac.cn
[5]e-mail: wfuzhang@opt.ac.cn

Received 27 August 2020; revised 10 November 2020; accepted 22 November 2020; posted 22 November 2020 (Doc. ID 408612); published 24 December 2020

Soliton microcombs (SMCs) are spontaneously formed in a coherently pumped high-quality microresonator, which provides a new tool for use as an on-chip frequency comb for applications of high-precision metrology and spectroscopy. However, generation of SMCs seriously relies on advanced experimental techniques from professional scientists. Here, we experimentally demonstrate a program-controlled single SMC source where the intracavity thermal effect is timely balanced using an auxiliary laser during single SMC generation. The microcomb power is adopted as the criteria for microcomb states discrimination and a forward and backward thermal tuning technique is employed for the deterministic single SMC generation. Further, based on a closed-loop control system, the repetition rate stability of the SMC source improved more than 20 times and the pump frequency can be continuously tuned by simply changing the operation temperature. The reliability of the SMC source is verified by consecutive 200 generation trials and maintaining over 10 h. We believe the proposed SMC source will have significant promising influences in future SMC-based application development.

https://doi.org/10.1364/PRJ.408612

1. INTRODUCTION

Kerr solitons are spontaneously organized when a high-quality microresonator is pumped by a continuous wave laser at a red-detuned regime, where double balances, cavity dissipation, and parametric gain as well as nonlinearity and dispersion, are reached [1–5]. A soliton microcomb (SMC) provides a route to a low-noise, ultrashort pulse with an over two orders of magnitude higher repetition rate compared to traditional approaches and high coherent frequency lines across the whole spectral coverage [2]. Single SMC is especially characterized by a smooth sech^2 spectrum envelope or an exactly equal pulses period. To date, SMCs have exhibited unprecedented performance in molecular spectroscopy [6–8], ranging measurement [9–11], microwave generation [12–14], optical frequency synthesis [15], classical and quantum communication systems [16–18] as well as in an optical atomic clock [19].

Deterministic and reliable generation of single SMC is fundamental and critical to develop SMC-based practical applications. Generally, SMCs evolve from a modulational instability (MI) comb when a pump laser sweeps across the resonance from a blue- to a red-detuned regime, which accompanies a dramatic decrease of intracavity power. The resonances of the microcavity will blue-shift due to thermo-optic effect, which hinders the pump stabilization in the soliton existing range (SER). To overcome the thermo-optic effect, several advanced experimental techniques have been developed, such as pump frequency scanning [20–26], a thermal tuning technique [27,28], chirped modulation [29], power kicking [30–32], self-injected locking [33,34], and auxiliary laser-assisted thermal balance [35–37]. However, due to the inherent stochasticity of intracavity dynamics, the quantity and location of spontaneously organized solitons are random [38,39]. To realize deterministic single SMC generation, frequency or thermal backward-tuning methods are introduced that use the thermo-optic effect induced nondegenerate character of the SER lower boundary. Although great progress has been achieved during the past several years, the generation of a single SMC still seriously relies on professional scientists or technicians. The widespread application of SMCs faces great challenges compared to mode-locked lasers, which offer two types of generation, either self-starting or program-controlled [40–43]. Therefore, automatic generation or a "one-button

start" SMC source is highly desirable to move SMC from in-lab, proof-of-concept experiments to industrial applications.

In this paper, we experimentally demonstrate program-controlled single SMC generation in a butterfly packaged high-index doped silica glass microring resonator (MRR). An auxiliary laser is introduced to realize intracavity thermal balance during the SMC generation, which releases the requirement of pump frequency or thermal tuning speed. And the microcomb states are discriminated by the optical power of the generated Kerr microcombs. Through optimizing the scanning steps of the operation temperature and pump frequency, a single SMC can be stably generated and its reliability is verified by 200 consecutive trials of single SMC generation. Further, using a feedback system, the repetition rate fluctuation is reduced by 20 times, which maintains a single SMC source for a long time. Finally, the pump wavelength is swept by 8 GHz through simply decreasing the operation temperature. Our experiment approaches a "one-button start" single SMC source, which would be a significant step for future-oriented SMC-based applications.

2. PRINCIPLE

Figure 1(a) shows the schematic of program-controlled single SMC source. A controller (e.g., a computer) is employed to acquire the microcomb data, discriminate the microcomb state, and tune the pump condition. The thermal relaxation response time of most microcavity platforms is in the magnitude of microseconds, which is out of the response time of an electrical control system, including the microcomb data acquisition time, microcomb state judge discrimination time, and communication time, as well as the execution time of a pump laser or thermal controller. Further, it is still a challenge to realize an instant response for a time-sharing operation system. The most frequently used schemes for SMC generation (e.g., pump frequency scanning and power kicking) require exact control time sequences, with a precision that is on the level of thermal relaxation time. Therefore, a tuning speed independent method is important for program-controlled single SMC generation. An auxiliary laser-assisted thermal balance method was recently developed, which not only timely realizes the intracavity thermal balance, but also extends the SER. An auxiliary laser is counter coupled into the microcavity, which acts as a negative feedback source to keep the intracavity optical power. Figure 1(b) schematically shows the intracavity power variation while the pump sweeps across a resonance. The dramatic pump power decrease is well compensated by the auxiliary laser during the SMC formation. Therefore, the auxiliary laser-assisted thermal balance method is tuning-speed independent, which satisfies the prerequisite of a program-controlled single SMC generation. Further, due to the inherently stochastic dynamics of SMC formation, the number and distribution of solitons are always random. Fortunately, it was proven that a single SMC can be stably obtained when solitons annihilate step by step through slowly backward tuning the pump frequency or the operation temperature, which benefits from the nondegeneration lower boundary of the SER due to thermo-optic effect, as shown in Fig. 1(c). An appropriate discrimination criterion is

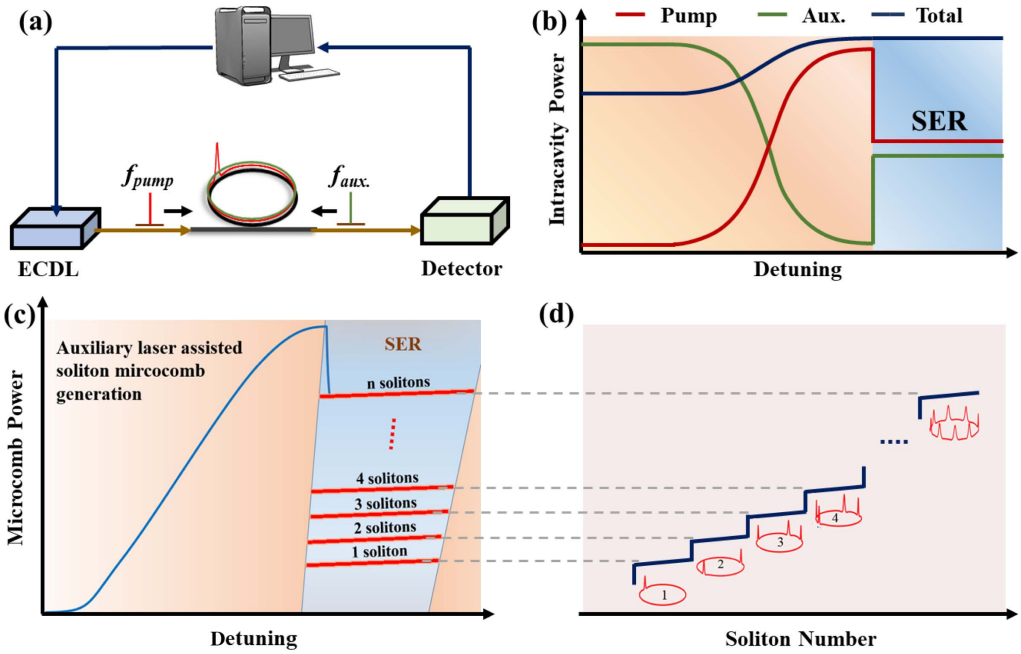

Fig. 1. Schematic of program-controlled single SMC generation. (a) Diagram of program-controlled single SMC generation. A controller is used for microcomb data acquisition, microcomb states discrimination, and pump condition adjustment. An auxiliary laser is counter coupled into the cavity to stabilize the intracavity power for tuning speed independent single SMC generation. (b) Diagram of the intracavity power evolution while the pump laser sweeps across the peak of resonance. (c) The lower boundary of the soliton existing range is nondegenerate while backward tuning the pump frequency or microcavity operation temperature, which provides an effective approach for deterministic soliton switching. (d) The soliton steps when intracavity solitons annihilate one by one. All the solitons have similar power under the same pump condition, which provides a simple soliton state discrimination criterion for program-controlled single SMC generation. ECDL: external cavity diode laser.

crucial for high-efficiency, program-controlled single SMC generation. For traditional mode-locked lasers, the temporal waveforms, radio-frequency spectra, or optical spectra are generally used to judge the laser operation states. However, for generation of SMC in the microcavity, this method encounters a great challenge for microcomb state discrimination because of the ultrahigh repetition rate that is beyond the bandwidth of currently available commercial photoelectric detectors and electronic devices. Intuitively, the microcomb states can also be distinguished by the optical spectral envelope, which is generally used in current microcomb generation experiments. But, it is time-consuming to acquire and recognize microcomb optical spectra. Meanwhile, the large volume of an optical spectrum analyzer (OSA) goes against miniaturized integration. It is noted that the microcomb power has a dramatical decrease, which can be used to judge the entrance of the SMC state. Meanwhile, all the solitons in a microresonator could have similar power under the same pump condition, which results in a series of soliton steps along with the annihilation of solitons, as schematically shown in Fig. 1(d). Therefore, the single soliton microcomb has the lowest power, which discriminates it from other soliton microcomb states. In our experiments, the microcomb power is used as the discrimination criterion of microcomb state. Compared to the optical spectrum measurements, it has the advantages of a higher detection speed and a simpler discrimination algorithm.

3. EXPERIMENTS AND RESULTS

Figure 2(a) presents the experimental setup for program-controlled single SMC generation. The core device is an add-drop microring resonator (MRR) that is fabricated on a CMOS-compatible, high-index doped silica glass platform, as shown in Fig. 2(c). The Q-factor and free spectral range (FSR) of the MRR are 1.7×10^6 and 49 GHz, respectively. The MRR is coupled with a standard eight-channel fiber array with a coupling loss of 2 dB per facet, and packaged into a 14-pin butterfly package with a TEC chip, as shown in Fig. 2(b). An auxiliary laser is counter-coupled into the MRR at the through port to realize thermal balance during the SMC generation. Two circulators are used to prevent the residual light from being injected into the EDFAs. The microcomb is measured at the drop port of the MRR. A part of the SMC spectrum is filtered out for SMC power monitor to avoid the influence of the pump and auxiliary lasers. A computer program is employed to control the SMC generation process. The microcomb power is read out from a power meter using a GPIB cable and compared to the criteria for different microcomb states discrimination. The operational orders are sent out for pump wavelength and operation temperature adjustment. Figure 2(d) presents the flow chart of a single SMC generation control program. In our experiments, both the pump and auxiliary lasers are boosted to 850 mW using two commercial EDFAs, corresponding to an on-chip power of ~425 mW (considering the waveguide coupling loss, and the insertion loss of polarization controllers and circulators). The spectrum range from 1542.5 nm to 1557.5 nm is filtered out for the microcomb power measurement. A real-time intracavity thermal balance is the prerequisite for program-controlled SMC generation. Therefore, in the initialization phase, the frequency spacing of the pump and auxiliary lasers should be carefully optimized. First, the pump wavelength is fixed at

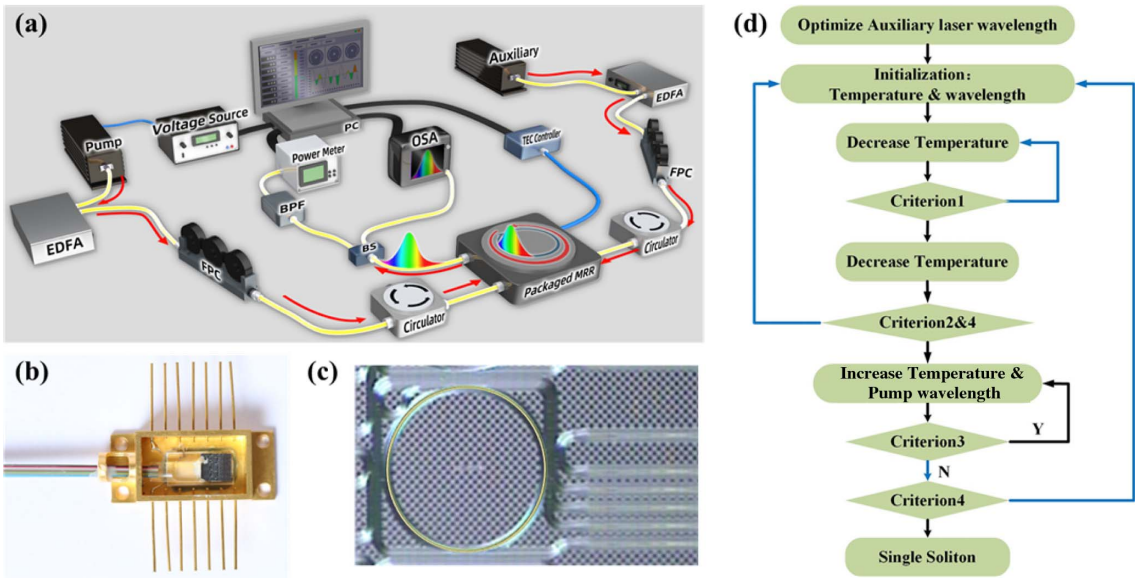

Fig. 2. Experimental setup. (a) Experimental setup of program-controlled single SMC generation. An auxiliary laser assisted thermal balance scheme is employed for tuning speed independent single SMC generation. The microcomb states are discriminated by the microcomb power, and the pump condition is exactly controlled by a computer program. EFDA: erbium doped fiber amplifier; FPC: fiber polarization control; TEC: thermoelectric cooler; OSA: optical spectrum analyzer; BPF: band pass filter; and PC: personal computer. (b) A 14-pin butterfly packaged MRR device whose operation temperature can be precisely tuned using an external TEC controller. (c) Microscope image of the 49 GHz high-index doped silica glass microring resonators. (d) Flowchart of the control program. There are four microcomb power criteria for different microcomb states discrimination.

1560.2 nm and the TEC is empirically initialized to ~55°C. According to the experimental experience, the wavelength of the auxiliary laser should be in the range between 1562.970 nm and 1562.975 nm for the resonance of 7FSR away from the pump. In the initialization phase, the program iterates an auxiliary wavelength with a step of 0.5 pm to check if a soliton step can be detected, which is confirmed by a more than 2 dB microcomb power decrease, but it is still higher than −12 dBm. The wavelength that reaches soliton steps is recorded as the initialization wavelength. For example, the pump and auxiliary lasers are initialized to 1560.2 nm and 1562.972 nm, respectively, and the temperature is initialized to 55°C to ensure the pump and auxiliary lasers locate at the blue-detuned side of relevant resonances.

Discrimination criterion based on microcomb power is the other key point for program-controlled single SMC generation. During the single SMC generation process, there are four typical microcomb states: pump out of resonance, modulational instability microcomb, multiple SMC, and single SMC. Discrimination criterion 1 is used to judge if a microcomb is formed. At the initial condition, both the pump and auxiliary lasers are out of resonance and the measured microcomb power is lower than −50 dBm. When the pump and auxiliary lasers are coupled into the MRR, new frequencies will be generated by FWM effect and the measured microcomb pump power increases up to −40 dBm [state I, Fig. 3(a)]. Once the pump power increases above the OPO threshold, the measured power will dramatically increase up to 0 dBm, which indicates the formation of microcombs [state II, Fig. 3(a)]. The power from −30 dBm to 0 dBm can be used as discrimination criterion 1. We choose the median value of −15 dBm as criterion 1 in our experiments. Criterion 2 acts as the SMC formation discrimination criterion. When the microcomb enters into an SMC state, the microcomb power will dramatically drop more than

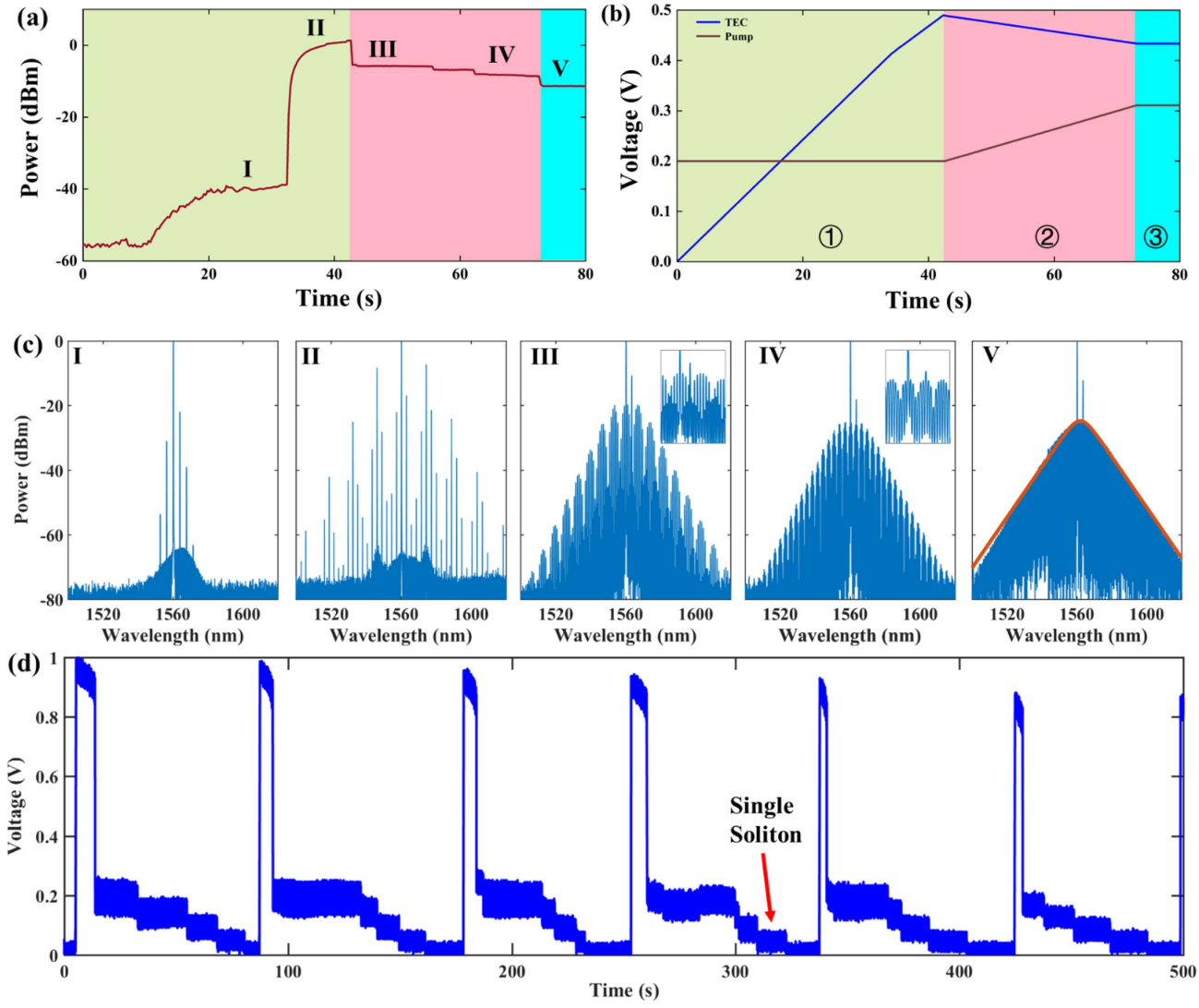

Fig. 3. Experimental results of program-controlled SMC generation. (a) The measured power trace of microcomb evolutionary process. The power of a single SMC is clamped in a range between −12 and −10 dBm. (b) The control signal waveforms of the TEC operation temperature and pump frequency. ① Forward tuning for microcomb generation. ② Backward tuning for deterministic single SMC generation. ③ Single SMC. (c) The typical optical spectra of different microcomb states. I, FWM frequency lines; II, modulational instability microcomb; III, four solitons; IV, two solitons; and V, single soliton. (d) The oscilloscope measured microcomb power trace when the program consecutively recycles.

3 dB [State III, Fig. 3(a)]. Meanwhile, the measured microcomb power should be higher than −12 dBm to ensure the pump is still in resonance. Therefore, a power variation more than 3 dB (criterion 2) and a microcomb power higher than −12 dBm (criterion 4) could be satisfied simultaneously for the SMC formation criterion. Once multiple SMCs are formed, soliton switching can be realized through backward tuning the operation temperature and forward tuning the pump wavelength. The intracavity solitons are annihilated step by step, which results in the optical power dropping in a down staircase fashion [States III to V, Fig. 3(a)]. Single SMC is recognized in the optical power range of −12 to −10 dBm (criterion 4 and criterion 3, respectively). The single SMC is verified by the smooth spectrum envelope with a sech^2 shape, as well as the lowest power step in the SMC power trace. In addition, the energy conversion efficiency of a single SMC is about 2.59% according to the experimental result, which is similar to the SMC generation scheme with a single pump. When the microcomb power drops below −12 dBm, the program will auto-reset and recycle to a new tuning round. It is noted that the optical power is obtained through averaging ten sampling values for each temperature adjustment step in our experiment.

Figure 3(a) shows the typical microcomb power trace, and Fig. 3(b) presents the control signals of the TEC and pump laser. The microcomb experiences FWM frequency lines (I), MI comb (II), and SMC states (III–V). At the first two stages, only the TEC operation temperature is forward tuned [prasinus colored in Fig. 3(b)] to increase the detuning of the lasers. The setting voltage of the TEC controller is tuned at a slope of 12.0 mV/s for State I and 9.1 mV/s for State II, respectively. When an SMC is obtained, the TEC operation temperature is backward tuned [red colored in Fig. 3(b)] and the pump wavelength is simultaneously swept to a longer wavelength. The tuning speed is optimized to 1.8 mV/s for a TEC setting voltage and 3.6 mV/s for a pump frequency control signal. The SMC power will decrease step by step up to the range of −12 dBm to −10 dBm, which falls into the single SMC discrimination criterion. Figure 3(c) shows the typical optical spectra of different microcomb states. Figure 3(d) presents the microcomb power trace of six consecutive single SMC generations by resetting the program when a single SMC is obtained. To check the reliability of the system, the single SMC generation process is repeated 200 times and the final microcomb state is confirmed by recognizing the measured optical spectra. The program is terminated at a single SMC state for all 200 trials, where 190 trials reach single SMC in one tuning round and the other 10 trials employ double tuning rounds. Further, we repeat the proposed system from a cold "off" state, and a single SMC is successfully generated in 20 consecutive trials.

We further studied the performance of the generated single SMC. Once the SMC is formed, the auxiliary laser will be modulated by the SMC and it forms a cross-phase modulated comb. Meanwhile, a part of the auxiliary laser is reflected back and co-propagates with the pump in the MRR, which will induce new frequency lines generation due to the FWM effect, as shown in Fig. 3(c). The beating of the SMC and new frequency lines will form an RF signal, as shown in Fig. 4(a). The fundamental frequency equals the frequency spacing between the auxiliary laser and the microcomb line within the same resonance. In time domain, it represents a slight power vibration, as shown in Fig. 4(b). The vibration amplitude is less than one percent, which has little effect in the application. In our experiments, the beating frequency can be tuned from 60 MHz to 150 MHz, which represents the maximum frequency fluctuation tolerance of the pump and auxiliary lasers to generate and maintain an SMC. On a long time scale, the laser frequency drifting will cause a loss of mode locking. Therefore, a feedback control would be significant for application development. Further, it is observed that repetition rate of a single SMC is linearly changing with the beating frequency at a rate of 2.91×10^{-3}. Therefore, the beating frequency stabilization is meaningful for SMC repetition rate stabilization. To verify the feasibility in principle, the beating frequency is directly detected by a high-speed PD and measured using an electrical spectrum analyzer (ESA). The beating frequency is read out and used as a feedback signal to control the frequency of the auxiliary laser. Meanwhile, the repetition rate of a single SMC is monitored by a PD (70 GHz) and an ESA (50 GHz). During the experiment, the TEC setting value is fixed and the pump frequency is tuned to maintain the SMC power. Figures 4(c) and 4(d) show the repetition rate variation of single SMC in one hour without and with the beating frequency locking, respectively. The repetition rate fluctuation is still reduced by more than 20 times. The tuning period is about 1.5 s in the test, and a higher control frequency will be helpful to further improve the repetition rate stability. Once the closed-loop control system works, single SMC can survive a whole work day (10 h). The experiments show the high

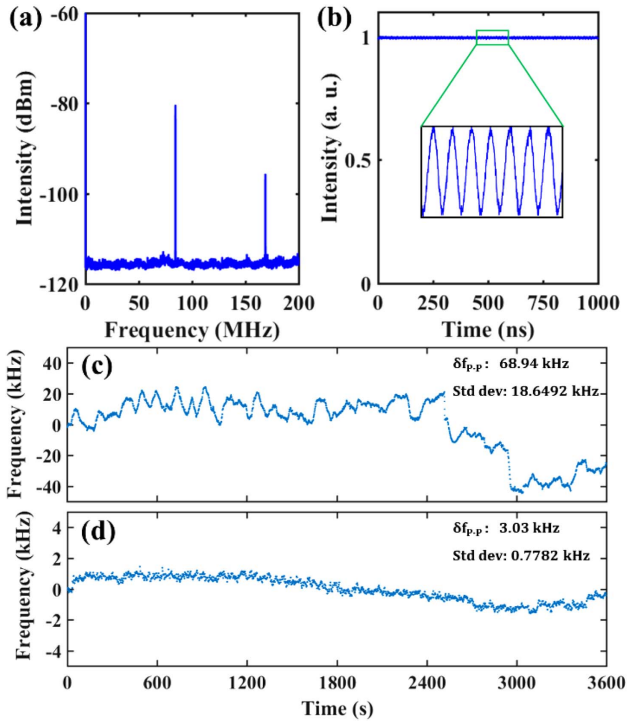

Fig. 4. Performance of a single SMC. (a) The radio frequency spectrum. (b) The waveform of a single SMC, which has an intensity modulation of approximately 1%. (c) and (d) The repetition rate fluctuation of single SMC without and with the beating frequency locking, respectively.

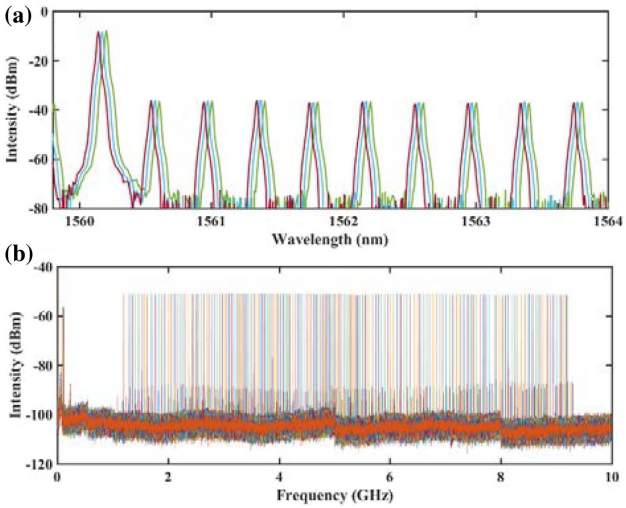

Fig. 5. Frequency shift of a single SMC. (a) The overlap optical spectra of a single SMC with frequency shift. (b) The beating RF spectra of the pump and reference lasers.

reliability of the program-controlled single SMC source, which could benefit SMC-based application development.

The SMC has a significant application value in spectroscopy. However, the ultrahigh repetition rate of an SMC may induce a loss of spectrum information. Therefore, a robust SMC frequency sweeping method is highly demanded in such applications. The proposed program-controlled SMC source has an inherent advantage for wavelength sweeping. When a single SMC is stabilized, SMC frequency sweeping can be simply realized by decreasing the operation temperature through control of the TEC setting value. The decrease in the operation temperature induces a blue shift of the resonance, and then the pump and auxiliary lasers will be autotuned to maintain the SMC power and beating frequency, respectively. To monitor the pump frequency shift, a reference laser whose wavelength is fixed at 1560.2 nm is employed. The beating signal of reference and the SMC is detected by a high-speed PD and measured by an ESA. While the operation temperature is tuned from 36.9°C to 33.4°C (thermistor from 6.0177 to 6.906 Ohm), the pump frequency is shifted by 8 GHz with step of about 5 MHz. Figures 5(a) and 5(b) are the overlap optical spectra and beating RF spectra, respectively. The frequency shift is limited by the pump laser used in our experiment. We believe the frequency shift can be further extended using a pump with a larger frequency tuning range.

4. DISCUSSION

We believe that a program-controlled and miniaturization SMC source is preferred and superior in future-oriented engineering and scientific applications. Our scheme employs microcomb power as the discrimination criterion for microcomb states. Compared to optical spectrum recognition, optical power discrimination criterion takes the merits of high-efficiency data acquisition and a simple microcomb states recognition algorithm. The simple control program can be realized in a microprocessor that has the potential of miniaturized integration. Meanwhile, the closed-loop program-controlled SMC source provides a route to actively capture the SMC by maintaining the microcomb power as well as the frequency spacing between the pump and auxiliary lasers. The automatic generation and capture of a single SMC will be very significant for future practical application development. The time consumed for a single tuning round is about 80 s, which is mainly caused by the relatively slow response time of TEC. In our experiments, the program waits ~200 ms for temperature stabilization at each tuning step. A faster temperature adjuster such as a microheater with a millisecond response time, or fast frequency lasers would be very helpful to shorten the single SMC generation time to just seconds. A real-time program system also can be employed to further shorten the single SMC generation time. On the other hand, the polarization states have significant influence on the effective power of the pump and auxiliary lasers for SMC generation. Due to the single-mode fiber used in our experiments, the polarization controllers should be carefully tuned and all the fiber is fixed on the platform to ensure the stability of the polarization states. In future-oriented applications, polarization-maintaining fiber can be employed to increase the robustness of program-controlled SMC source.

5. CONCLUSION

In conclusion, a program-controlled single SMC source is demonstrated in a high-index doped silica glass MRR. Optical power is used as microcomb state discrimination criterion that benefits the high-efficiency and simple system. Using microcomb power and the beating frequency of an auxiliary laser and SMC as feedback signals, the repetition rate stability of the single SMC is improved 20 times. The frequency of the single SMC source is shifted by 8 GHz by simply tuning the operation temperature. The proposed single SMC source showed high reliability in 200 consecutive trials and during an experiment where it was maintained for 10 h. Together with ultrahigh-quality microcavities, the scheme would approach a miniaturization integrated smart SMC source, which will play a significant role in future practical applications.

Funding. National Natural Science Foundation of China (61635013, 61675231); National Key Research and Development Program of China (2019YFA0308200); Strategic Priority Research Program of the Chinese Academy of Sciences (XDB24030600).

Acknowledgment. The authors thank Liujun Guo for helpful discussions.

Disclosures. The authors declare no conflicts of interest.

REFERENCES

1. P. Grelu and N. Akhmediev, "Dissipative solitons for mode-locked lasers," Nat. Photonics **6**, 84–92 (2012).
2. M. E. Fermann and I. Hartl, "Ultrafast fibre lasers," Nat. Photonics **7**, 868–874 (2013).
3. F. Leo, S. Coen, P. Kockaert, S.-P. Gorza, P. Emplit, and M. Haelterman, "Temporal cavity solitons in one-dimensional Kerr media as bits in an all-optical buffer," Nat. Photonics **4**, 471–476 (2010).

4. T. J. Kippenberg, A. L. Gaeta, M. Lipson, and M. L. Gorodetsky, "Dissipative Kerr solitons in optical microresonators," Science **361**, eaan8083 (2018).
5. W. Wang, L. Wang, and W. Zhang, "Advances in soliton microcomb generation," Adv. Photon. **2**, 034001 (2020).
6. N. Picqué and T. W. Hänsch, "Frequency comb spectroscopy," Nat. Photonics **13**, 146–157 (2019).
7. M.-G. Suh, Q.-F. Yang, K. Y. Yang, X. Yi, and K. J. Vahala, "Microresonator soliton dual-comb spectroscopy," Science **354**, 600–603 (2016).
8. A. Dutt, C. Joshi, X. Ji, J. Cardenas, Y. Okawachi, K. Luke, A. L. Gaeta, and M. Lipson, "On-chip dual-comb source for spectroscopy," Sci. Adv. **4**, e1701858 (2018).
9. J. Riemensberger, A. Lukashchuk, M. Karpov, W. Weng, E. Lucas, J. Liu, and T. J. Kippenberg, "Massively parallel coherent laser ranging using a soliton microcomb," Nature **581**, 164–170 (2020).
10. M.-G. Suh and K. J. Vahala, "Soliton microcomb range measurement," Science **359**, 884–887 (2018).
11. J. Wang, Z. Lu, W. Wang, F. Zhang, J. Chen, Y. Wang, X. Zhao, J. Zheng, S. T. Chu, W. Zhao, B. E. Little, X. Qu, and W. Zhang, "Long-distance ranging with high precision using a soliton microcomb," Photon. Res. **8**, 1964–1972 (2020).
12. J. Liu, E. Lucas, A. S. Raja, J. He, J. Riemensberger, R. N. Wang, M. Karpov, H. Guo, R. Bouchand, and T. J. Kippenberg, "Photonic microwave generation in the X- and K-band using integrated soliton microcombs," Nat. Photonics **14**, 486–491 (2020).
13. W. Liang, D. Eliyahu, V. S. Ilchenko, A. A. Savchenkov, A. B. Matsko, D. Seidel, and L. Maleki, "High spectral purity Kerr frequency comb radio frequency photonic oscillator," Nat. Commun. **6**, 7957 (2015).
14. M. Tan, X. Xu, B. Corcoran, J. Wu, A. Boes, T. G. Nguyen, S. T. Chu, B. E. Little, R. Morandotti, A. Mitchell, and D. J. Moss, "Microwave and RF photonic fractional Hilbert transformer based on a 50 GHz Kerr micro-comb," J. Lightwave Technol. **37**, 6097–6104 (2019).
15. D. T. Spencer, T. Drake, T. C. Briles, J. Stone, L. C. Sinclair, C. Fredrick, Q. Li, D. Westly, B. R. Ilic, A. Bluestone, N. Volet, T. Komljenovic, L. Chang, S. H. Lee, D. Y. Oh, M.-G. Suh, K. Y. Yang, M. H. P. Pfeiffer, T. J. Kippenberg, E. Norberg, L. Theogarajan, K. Vahala, N. R. Newbury, K. Srinivasan, J. E. Bowers, S. A. Diddams, and S. B. Papp, "An optical-frequency synthesizer using integrated photonics," Nature **557**, 81–85 (2018).
16. B. Corcoran, M. Tan, X. Xu, A. Boes, J. Wu, T. G. Nguyen, S. T. Chu, B. E. Little, R. Morandotti, A. Mitchell, and D. J. Moss, "Ultra-dense optical data transmission over standard fibre with a single chip source," Nat. Commun. **11**, 2568 (2020).
17. F.-X. Wang, W. Wang, R. Niu, X. Wang, C.-L. Zou, C.-H. Dong, B. E. Little, S. T. Chu, H. Liu, P. Hao, S. Liu, S. Wang, Z.-Q. Yin, D.-Y. He, W. Zhang, W. Zhao, Z.-F. Han, G.-C. Guo, and W. Chen, "Quantum key distribution with on-chip dissipative Kerr soliton," Laser Photon. Rev. **14**, 1900190 (2020).
18. P. Marin-Palomo, J. N. Kemal, M. Karpov, A. Kordts, J. Pfeifle, M. H. P. Pfeiffer, P. Trocha, S. Wolf, V. Brasch, M. H. Anderson, R. Rosenberger, K. Vijayan, W. Freude, T. J. Kippenberg, and C. Koos, "Microresonator-based solitons for massively parallel coherent optical communications," Nature **546**, 274–279 (2017).
19. S. B. Papp, K. Beha, P. Del'Haye, F. Quinlan, H. Lee, K. J. Vahala, and S. A. Diddams, "Microresonator frequency comb optical clock," Optica **1**, 10–14 (2014).
20. T. Herr, V. Brasch, J. D. Jost, C. Y. Wang, N. M. Kondratiev, M. L. Gorodetsky, and T. J. Kippenberg, "Temporal solitons in optical microresonators," Nat. Photonics **8**, 145–152 (2014).
21. H. Guo, M. Karpov, E. Lucas, A. Kordts, M. H. P. Pfeiffer, V. Brasch, G. Lihachev, V. E. Lobanov, M. L. Gorodetsky, and T. J. Kippenberg, "Universal dynamics and deterministic switching of dissipative Kerr solitons in optical microresonators," Nat. Phys. **13**, 94–102 (2017).
22. T. Wildi, V. Brasch, J. Liu, T. J. Kippenberg, and T. Herr, "Thermally stable access to microresonator solitons via slow pump modulation," Opt. Lett. **44**, 4447–4450 (2019).
23. J. R. Stone, T. C. Briles, T. E. Drake, D. T. Spencer, D. R. Carlson, S. A. Diddams, and S. B. Papp, "Thermal and nonlinear dissipative-soliton dynamics in Kerr-microresonator frequency combs," Phys. Rev. Lett. **121**, 063902 (2018).
24. J. Liu, H. Tian, E. Lucas, A. S. Raja, G. Lihachev, R. N. Wang, J. He, T. Liu, M. H. Anderson, W. Weng, S. A. Bhave, and T. J. Kippenberg, "Monolithic piezoelectric control of soliton microcombs," Nature **583**, 385–390 (2020).
25. S. Wan, R. Niu, Z.-Y. Wang, J.-L. Peng, M. Li, J. Li, G.-C. Guo, C.-L. Zou, and C.-H. Dong, "Frequency stabilization and tuning of breathing solitons in Si_3N_4 microresonators," Photon. Res. **8**, 1342–1349 (2020).
26. H.-J. Chen, Q.-X. Ji, H. Wang, Q.-F. Yang, Q.-T. Cao, Q. Gong, X. Yi, and Y.-F. Xiao, "Chaos-assisted two-octave-spanning microcombs," Nat. Commun. **11**, 2336 (2020).
27. C. Joshi, J. K. Jang, K. Luke, X. Ji, S. A. Miller, A. Klenner, Y. Okawachi, M. Lipson, and A. L. Gaeta, "Thermally controlled comb generation and soliton modelocking in microresonators," Opt. Lett. **41**, 2565–2568 (2016).
28. W. Wang, Z. Lu, W. Zhang, S. T. Chu, B. E. Little, L. Wang, X. Xie, M. Liu, Q. Yang, L. Wang, J. Zhao, G. Wang, Q. Sun, Y. Liu, Y. Wang, and W. Zhao, "Robust soliton crystals in a thermally controlled microresonator," Opt. Lett. **43**, 2002–2005 (2018).
29. D. C. Cole, J. R. Stone, M. Erkintalo, K. Y. Yang, X. Yi, K. J. Vahala, and S. B. Papp, "Kerr-microresonator solitons from a chirped background," Optica **5**, 1304–1310 (2018).
30. X. Yi, Q.-F. Yang, K. Y. Yang, M.-G. Suh, and K. Vahala, "Soliton frequency comb at microwave rates in a high-*Q* silica microresonator," Optica **2**, 1078–1085 (2015).
31. V. Brasch, M. Geiselmann, M. H. P. Pfeiffer, and T. J. Kippenberg, "Bringing short-lived dissipative Kerr soliton states in microresonators into a steady state," Opt. Express **24**, 29312–29320 (2016).
32. X. Yi, Q.-F. Yang, K. Youl Yang, and K. Vahala, "Active capture and stabilization of temporal solitons in microresonators," Opt. Lett. **41**, 2037–2040 (2016).
33. B. Shen, L. Chang, J. Liu, H. Wang, Q.-F. Yang, C. Xiang, R. N. Wang, J. He, T. Liu, W. Xie, J. Guo, D. Kinghorn, L. Wu, Q.-X. Ji, T. J. Kippenberg, K. Vahala, and J. E. Bowers, "Integrated turnkey soliton microcombs," Nature **582**, 365–369 (2020).
34. N. G. Pavlov, S. Koptyaev, G. V. Lihachev, A. S. Voloshin, A. S. Gorodnitskiy, M. V. Ryabko, S. V. Polonsky, and M. L. Gorodetsky, "Narrow-linewidth lasing and soliton Kerr microcombs with ordinary laser diodes," Nat. Photonics **12**, 694–698 (2018).
35. H. Zhou, Y. Geng, W. Cui, S.-W. Huang, Q. Zhou, K. Qiu, and C. W. Wong, "Soliton bursts and deterministic dissipative Kerr soliton generation in auxiliary-assisted microcavities," Light Sci. Appl. **8**, 50 (2019).
36. R. Niu, S. Wan, S.-M. Sun, T.-G. Ma, H.-J. Chen, W.-Q. Wang, Z.-Z. Lu, W.-F. Zhang, G.-C. Guo, C.-L. Zou, and C.-H. Dong, "Repetition rate tuning of soliton in microrod resonators," arXiv:1809.06490 (2018).
37. Z. Lu, W. Wang, W. Zhang, S. T. Chu, B. E. Little, M. Liu, L. Wang, C.-L. Zou, C.-H. Dong, B. Zhao, and W. Zhao, "Deterministic generation and switching of dissipative Kerr soliton in a thermally controlled micro-resonator," AIP Adv. **9**, 025314 (2019).
38. X. Yi, Q.-F. Yang, K. Y. Yang, and K. Vahala, "Imaging soliton dynamics in optical microcavities," Nat. Commun. **9**, 3565 (2018).
39. X. Xue, X. Zheng, and B. Zhou, "Soliton regulation in microcavities induced by fundamental-second-harmonic mode coupling," Photon. Res. **6**, 948–953 (2018).
40. U. Andral, R. Si Fodil, F. Amrani, F. Billard, E. Hertz, and P. Grelu, "Fiber laser mode locked through an evolutionary algorithm," Optica **2**, 275–278 (2015).
41. G. Pu, L. Yi, L. Zhang, and W. Hu, "Intelligent programmable mode-locked fiber laser with a human-like algorithm," Optica **6**, 362–369 (2019).
42. G. B. Rieker, F. R. Giorgetta, W. C. Swann, J. Kofler, A. M. Zolot, L. C. Sinclair, E. Baumann, C. Cromer, G. Petron, C. Sweeney, P. P. Tans, I. Coddington, and N. R. Newbury, "Frequency-comb-based remote sensing of greenhouse gases over kilometer air paths," Optica **1**, 290–298 (2014).
43. M. Liu, R. Tang, A.-P. Luo, W.-C. Xu, and Z.-C. Luo, "Graphene-decorated microfiber knot as a broadband resonator for ultrahigh-repetition-rate pulse fiber lasers," Photon. Res. **6**, C1–C7 (2018).